JOURNAL OF Materials CHEMISTRY

Synthesis, characterization and photocatalytic activity of $ZnFe_2O_4/TiO_2$ nanocomposite

Zhi-hao Yuan*[a,b] and Li-de Zhang[b]

[a]*Department of Physics, Tsinghua University, Beijing 100084, China. E-mail: zhyuan@tsinghua.edu.cn*
[b]*Institute of Solid State Physics, Chinese Academy of Sciences, Hefei 230031, China*

Received 29th August 2000, Accepted 15th January 2001
First published as an Advance Article on the web 16th February 2001

A new nanocomposite material $ZnFe_2O_4/TiO_2$ is prepared by a colloid chemistry method and characterized through X-ray diffraction (XRD) and transmission electron microscopy. The corresponding photocatalytic activity in the mineralization of phenol is evaluated in comparison with pure $ZnFe_2O_4$ and TiO_2 nanomaterials. From XRD measurements, it is found that when annealed at relatively low temperature, $ZnFe_2O_4$ and TiO_2 crystallite phases in the composite separate from each other, and when annealed at high temperature a solid reaction between $ZnFe_2O_4$ and TiO_2 takes place. In addition, it is observed that the $ZnFe_2O_4$ nanoparticles seem to play a role in inhibiting the anatase-to-rutile phase transformation of TiO_2. According to the phenol degradation, the $ZnFe_2O_4/TiO_2$ nanocomposite is more effective as a photocatalyst than pure TiO_2, showing that the nanocomposite approach could be an excellent choice to improve the photoactivity of TiO_2.

Introduction

The applications of TiO_2-based materials in the photocatalytic oxidation of organic pollutants and in photoelectrochemical conversion of solar energy have been extensively studied in the past decades owing to its excellent (photo)chemical stability, low cost and non-toxicity.[1–8] However, for such applications titania exhibits at least two disadvantages: low photoactivity and poor efficiency in the conversion of solar energy.[4,9–11]

The low photoactivity of TiO_2 is thought to be due mainly to the fast recombination of photogenerated electrons and holes.[12,13] Several transition metal ion dopings in titania can promote the separation of photogenerated charge-carriers, and thus improve its photoactivity.[14–17] The addition of some oxides (*e.g.* SiO_2, WO_3, Al_2O_3, SnO_2, Nb_2O_5, *etc.*) to the TiO_2 matrix has been found to be beneficial for its photoactivity.[18–21] However, in most cases, such dopings or additions are unsuccessful.[22–24]

Titania, with a wide band-gap energy (anatase *ca.* 3.2 eV, rutile *ca.* 3.0 eV), is a UV absorber yet utilizes only a very small fraction of the solar spectrum ($<5\%$). There have been some successful efforts in improving the efficiency of using solar energy by organic dye sensitization:[4,25–28] among them, the first efficient example was reported by Grätzel and O'Regan[27] through a trimeric ruthenium complex dye, for which an efficiency of 12% was observed. However, from a practical point of view, it is necessary to increase the thermal- and photostability of organic sensitizers.[26,29] Recently, there has been an increasing interest in the use of inorganic sensitizers. A coupled semiconductor system consisting of TiO_2 and another semiconductor with a relatively small band-gap energy, such as CdS, CdSe, FeS_2 or RuS_2, can extend the photoresponse of TiO_2 into the visible range and thus increase its efficiency in utilizing solar energy.[30–33] Unfortunately, these sulfides and selenides are both sensitive to photoanodic corrosion.

Zinc ferrite ($ZnFe_2O_4$), with a spinel structure, is well known to be an anomalous antiferromagnetic substance as demonstrated in previous works.[34,35] Recent studies have shown that $ZnFe_2O_4$, with a relatively small band-gap[36] (*ca.* 1.9 eV), especially nanometer-sized $ZnFe_2O_4$, is a potentially useful solar energy material for photoelectric conversion and photochemical hydrogen production from water,[37–39] whose advantages are to absorb visible light and to not be sensitive to photoanodic corrosion. Since both $ZnFe_2O_4$ and TiO_2 are promising solar energy materials with respective advantages and disadvantages, it is expected that their nanocomposites should exhibit useful characteristics, making them suitable for far-reaching applications in photocatalysis and photoelectric conversion. Based on these considerations we studied the possibility of the preparation of a $ZnFe_2O_4/TiO_2$ nanocomposite. For the preparation of $ZnFe_2O_4$ and TiO_2 alone, many reports have been published.[40–46] Usually, the former is prepared in alkaline media, whereas the latter is carried out under acid conditions – the difficulty in synthesizing the nanocomposite results from this incompatibility in their preparation procedures. In a recent work, we have successfully synthesized the nanocomposite by surface modification of their respective nanoparticles using a surfactant. Preliminary results have shown that the $ZnFe_2O_4/TiO_2$ nanocomposite is a more effective photocatalyst for the photodegradation of organic compounds than TiO_2 alone.

Experimental

The colloid chemistry method was adopted to synthesize the $ZnFe_2O_4/TiO_2$ nanocomposite by the following procedure. First, the $ZnFe_2O_4$ and TiO_2 nanoparticles were prepared, respectively, by coprecipitation and controlled hydrolysis methods. Details of their preparations have been described elsewhere.[40,41] Briefly, $ZnFe_2O_4$ and TiO_2 were coprecipitated or precipitated, respectively, from a mixed solution of 0.1 mol dm^{-3} of $Zn(NO_3)_2$ and 0.2 mol dm^{-3} of $Fe(NO_3)_3$ at a pH value of 13 and at a temperature of 100 °C, or from a mixed solution with a volume ratio of $Ti(OC_4H_9)_4$: C_2H_5OH : $H_2O = 1:10:100$ at pH 2 under vigorous stirring. Both products were filtered and washed with deionized water, in sequence. Then they were introduced into 0.01 mol dm^{-3} dodecyl benzene sulfonic acid (DBS) under stirring, where $ZnFe_2O_4$ or TiO_2 nanoparticles were capped with a layer of DBS. (The capped $ZnFe_2O_4$ and TiO_2 nanoparticles are readily dispersed in organic solvents such as toluene and benzene,

DOI: 10.1039/b006994i

which are suitable for the composite materials.) The capped $ZnFe_2O_4$ and TiO_2 nanoparticles were mixed with various molar ratio mixtures of Zn : Ti = 0.01, 0.05, 0.1 and 0.2 in toluene under vigorous stirring, followed by extraction into toluene. The obtained organic phase was, in sequence, refluxed for 1 h, washed with deionized water several times, and distilled to remove the residual water. At the end of this process, a mixed organic sol of $ZnFe_2O_4/TiO_2$ was obtained. This sol was then distilled to remove the toluene solvent, followed by a heat-treatment at *ca.* 400 °C in air for 2 h to fire the DBS. Finally, the obtained $ZnFe_2O_4/TiO_2$ nanoparticles were annealed at different temperatures for 2 h. In addition, pure TiO_2 and $ZnFe_2O_4$ nanoparticles were also prepared by the same method for comparisons.

XRD measurement was performed with a Philips PW-1700 X-ray diffractometer with Cu-Kα incident radiation. The average crystallite sizes of the spinel phase of $ZnFe_2O_4$, and anatase as well as rutile phases of TiO_2, were estimated from the full width at half-maximum of their most intense diffraction peaks using Scherrer's formula. The particle morphology was observed by transmission electron microscopy (TEM; Jeol JEM-200CX). The compositions of the $ZnFe_2O_4/TiO_2$ nanocomposites were further characterized through inductively coupled plasma emission spectroscopy (IL-plasma 100), and the measurement results revealed that the molar ratios in the composites are approximatively equal to those of the original mixture.

The photocatalytic activity was evaluated by phenol photodegradation. Photocatalytic reaction was performed directly under sunlight irradiation using bubbled air instead of pure O_2. As there was found to be a variation in the sunlight intensity during irradiation, the photocatalytic apparatus was designed into a system with multiple parallel photoreactors. These parallel photoreactors were simultaneously used in order to ensure that the photocatalytic reactions were performed under identical irradiation conditions. One of the reactors was always loaded with undoped TiO_2 catalyst as a comparison. The reagents and conditions for the photocatalytic reactions were the same: 500 ml of the suspension, 0.5 g l^{-1} of photocatalyst, initial concentration of 5×10^{-4} mol l^{-1} phenol, and neutral pH solution; reactions lasted for several hours. Samples (*ca.* 5 ml) for analysis were withdrawn through pipettes and immediately centrifugated. The phenol concentration in the supernatant solution was determined by UV–Vis spectrophotometry (Cary-5E, $\lambda_{dec.}\approx270$ nm). Calibration was carried out using phenol solutions of known concentration.

Results and discussion

X-Ray diffraction analysis can provide detailed information on crystallite structure characteristics (*i.e.* crystallite phase formation and phase transformation). Fig. 1(a) gives the XRD pattern of $ZnFe_2O_4/TiO_2$ composite after annealing at 400 °C, a temperature at which the surfactants can just be fired. The XRD pattern shows the presence of TiO_2 (anatase phase) and $ZnFe_2O_4$ (spinel phase) with respective broad diffraction peaks. This indicates that in the composite, TiO_2 and $ZnFe_2O_4$ crystallite phases separate from each other. The broad peaks show that the crystallite size is small. According to Fig. 1(b) and 1(c), the rutile phase of TiO_2 in the composite begins to form at *ca.* 600 °C. This temperature is higher than that for the pure TiO_2 nanoparticles obtained by the sol–gel method.[42] This difference might be due to different preparation methods used or to the retarding effect on the anatase-to-rutile (A→R) transformation resulting from the presence of $ZnFe_2O_4$ nanoparticles in the composite, or both. From Fig. 1(d) and 1(e), it is noted that when the composite is annealed above *ca.* 700 °C, the strongest peak ($2\theta=25.3°$) of the anatase phase disappears, and simultaneously, the peaks of two new phases

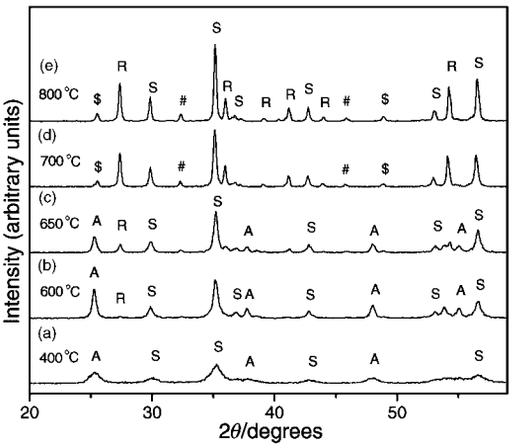

Fig. 1 XRD patterns of the $ZnFe_2O_4/TiO_2$ composite with a molar ratio of Zn : Ti = 0.1 after annealing at various temperatures for 2 h. (A = anatase; R = rutile; S = spinel; $ = Fe_2TiO_5; # = $ZnTiO_3$).

($ZnTiO_3$ and Fe_2TiO_5) appear in the XRD patterns. This shows that a solid reaction of $ZnFe_2O_4+2TiO_2\rightarrow ZnTiO_3+Fe_2TiO_5$ has taken place at the high annealing temperature.

The relations between the annealing temperature and the average grain size of these crystallite phases in the composite are tabulated in Table 1, together with those of pure TiO_2 and $ZnFe_2O_4$ samples for comparison. From Table 1, the following observations can be made:

(1) With an increase of the annealing temperature, the grain sizes of TiO_2 (including anatase and rutile) rapidly increase, especially when the A→R transformation occurs, whereas the $ZnFe_2O_4$ grains grow relatively slowly. This rapid increase of the grain size during the transformation is thought to be due to an enhancement of the A→R transformation in the TiO_2 grain growth.[47]

(2) In the composite, an increase in temperature has the same effect on the growth of $ZnFe_2O_4$ grains as it does on the ones of pure $ZnFe_2O_4$, while the growth rate of TiO_2 grains is obviously lower than that of the pure TiO_2. This suggests that the $ZnFe_2O_4$ component in the composite can play a role in inhibiting the grain growth of TiO_2.

TEM observations for a typical $ZnFe_2O_4/TiO_2$ composite after annealing at different temperatures are shown in Fig. 2. It can be seen that the TiO_2 and $ZnFe_2O_4$ crystallite particles in the composite are homogeneously dispersed, and with a increase of the annealing temperature, the particles grow with uniform sizes.

Fig. 3 gives the absorption spectra of phenol solution irradiated under sunlight in the presence of the $ZnFe_2O_4/TiO_2$ composite, pure $ZnFe_2O_4$, and pure TiO_2. The phenol photodegradation can be monitored from the absorption at *ca.* 270 nm. It is evident from Fig. 3 that the pure $ZnFe_2O_4$

Table 1 Variations of the grain size of the $ZnFe_2O_4/TiO_2$ composite with the molar ratio of Zn : Ti = 0.1, pure $ZnFe_2O_4$, and TiO_2 after annealing at different temperatures

	Mean grain size/nm					
	Composite			Pure TiO_2		$ZnFe_2O_4$
Temperature/°C	Anatase	Rutile	Spinel	Anatase	Rutile	Spinel
400	8.6	—[a]	7.7	10.7	—[a]	8.3
450	9.7	—[a]	8.9	12.4	—[a]	9.2
500	13.6	—[a]	10.5	15.9	—[a]	10.8
600	26	31	16.4	34	66	16.1
650	34	43	20.3	51	>100	19.5
700	—[a]	52	25.9	75	>100	24.8

[a] No phase present within the sample.

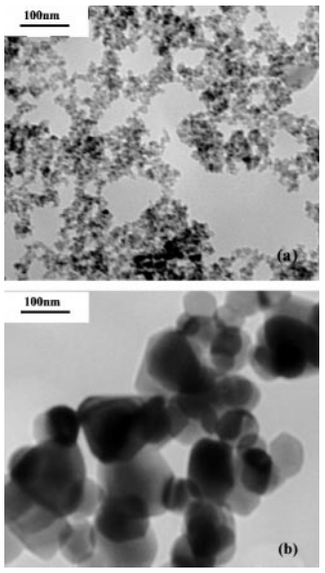

Fig. 2 TEM images of the $ZnFe_2O_4/TiO_2$ composite with a molar ratio of Zn : Ti = 0.1 after annealing at 400 °C (a) and 850 °C (b) for 2 h.

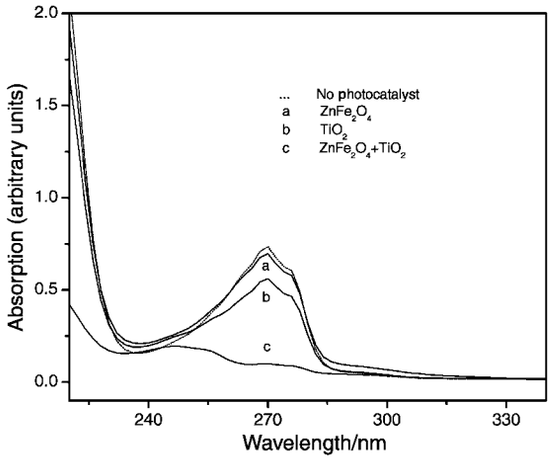

Fig. 3 Optical absorption spectra of phenol solutions after irradiation under sunlight for 3 h in the presence of (a) pure $ZnFe_2O_4$, (b) pure TiO_2 and (c) $ZnFe_2O_4/TiO_2$ composite with a molar ratio of Zn : Ti = 0.05.

nanoparticles have little photocatalytic activity for the phenol photodegradation, whereas pure TiO_2 nanoparticles, as well as $ZnFe_2O_4/TiO_2$ nanocomposite, are quite efficient photocatalysts. A careful investigation of the absorption spectra reveals that more than 95% of the phenol disappears within 3 h of irradiation when the composite photocatalyst is used, and in the case of TiO_2 alone, only *ca.* 20% of the phenol is photodecomposed within 3 h of irradiation. This shows that the $ZnFe_2O_4/TiO_2$ composite is more efficient than the pure TiO_2 for the phenol photodegradation. Fig. 4 shows the influence of the annealing temperature on the photoactivity of the $ZnFe_2O_4/TiO_2$ composite. It can be seen that the photoactivity obviously drops down with an increase in temperature. The decrease in the photoactivity is attributed to the increase of the grain size with increasing temperature. In addition, the photoactivity also depends on the composite composition. In our experiment, the best photoactivity was obtained with a molar ratio of Zn : Ti = 0.05.

The enhanced photoactivity of the $ZnFe_2O_4/TiO_2$ composite is not well understood. We think that this might be related to the following two factors. (1) The addition of $ZnFe_2O_4$ nanoparticles to TiO_2 can extend the photoresponse of TiO_2 toward the visible region, and thus increase the efficiency of utilizing solar energy. (2) In the composite, a coupled effect can exist between the $ZnFe_2O_4$ and TiO_2 energy bands due to some differences in their band-gap positions. This possible coupling effect can play a role in promoting the charge separation of the generated carriers and interfacial charge transfer, and therefore improve the photoactivity of TiO_2. Further works are underway.

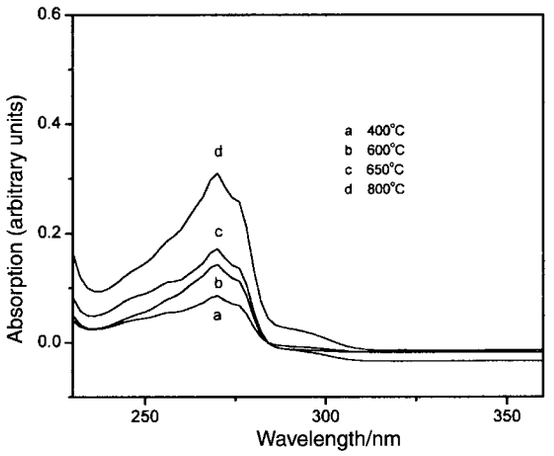

Fig. 4 Optical absorption spectra of phenol solutions in the presence of a $ZnFe_2O_4/TiO_2$ composite with a molar ratio of Zn : Ti = 0.05 after annealing at different temperatures for 2 h (irradiation for 3 h).

Conclusions

Nanocomposites consisting of zinc ferrite and titania have been successfully synthesized through colloid chemistry processing using a surfactant-capping technique. Application of these nanocomposites for the photocatalytic decomposition of phenol gives an increased photoactivity relative to TiO_2-only nanomaterials. The present results show that the $ZnFe_2O_4/TiO_2$ nanocomposite may be a promising solar energy material for applications in photocatalysis as well as in photoelectrochemical conversion.

Acknowledgements

Authors would like to thank Professor S. S. Fan, Professor Y. D. Li, Professor N. F. Gao, Dr L. Liu, Dr C. C. Tang, Professor G. H. Li, Professor Y. Qin, Mrs L. Cheng and Mr. K Zhen for their cooperation and help. The authors also thank Dr M. Lamy de la Chapelle for the improvement of the English. This work was supported by the State Key Project of Fundamental Research of China.

References

1 D. F. Olis, E. Pelizzetti and N. Serpone, *Environ. Sci. Technol.*, 1991, **25**, 1523.
2 A. L. Pruden and D. F. Ollis, *J. Catal.*, 1983, **82**, 404.
3 R. W. Matthews, *J. Phys. Chem.*, 1987, **91**, 3328.
4 J. R. Bolton, *Sol. Energy. Mater. Sol. Cells*, 1995, **38**, 543.
5 G. Hodes, I. D. Howell and L. Peter, *J. Electrochem. Soc.*, 1992, **139**, 3136.
6 S. Sodergren, A. Hagfeldt, J. Olsson and S. E. Lindquist, *J. Phys. Chem.*, 1994, **98**, 5552.
7 D. E. Scaife, *Sol. Energy*, 1980, **25**, 41.
8 M. Fugihira, Y. Satoh and T. Osa, *Nature*, 1981, **206**, 293.
9 K. Vinodgopal and P. V. Kamat, *Sol. Energy Mater. Sol. Cells*, 1995, **38**, 401.
10 A. Fujishima and K. Honda, *Nature*, 1972, **238**, 37.
11 H. Gerisher and A. Heller, *J. Phys. Chem.*, 1991, **95**, 5267.
12 W. Choi, A. Termin and M. R. Hoffmann, *Angew. Chem.*, 1994, **106**, 1148.
13 W. D. Ward and A. J. Bard, *J. Phys. Chem.*, 1982, **86**, 3599.

14 E. C. Butler and A. P. Davis, *J. Photochem. Photobiol., A*, 1993, **70**, 273.
15 W. Choi, A. Termin and M. R. Hoffmann, *J. Phys. Chem.*, 1994, **98**, 13 669.
16 A. Sclafani, L. Palmisano and E. Davi, *J. Photochem. Photobiol. A*, 1991, **61**, 269.
17 T. Y. Wei, Y. Y. Wang and C. C. Wan, *J. Photochem. Photobiol. A*, 1990, **55**, 115.
18 S. Hotchandani and P. V. Kamat, *J. Phys. Chem.*, 1992, **96**, 6834.
19 C. Anderson and A. J. Bard, *J. Phys. Chem. B*, 1997, **101**, 2611.
20 Y. R. Do, W. Lee. K. Dwight and A. Wold, *J. Solid State Chem.*, 1994, **108**, 198.
21 S. Okazaki and T. Oknyama, *Bull. Chem. Soc. Jpn.*, 1983, **56**, 2159.
22 S. T. Martin, C. L. Morrison and M. R. Hoffmann, *J. Phys. Chem.*, 1994, **88**, 13 695.
23 J. M. Herrmann, J. Disdier and P. Pichat, *Chem. Phys. Lett.*, 1984, **108**, 618.
24 A. Mills, R. H. Davies and D. Worsley, *Chem. Soc. Rev.*, 1993, **22**, 417.
25 H. Ross, J. Bending and S. Hecht, *Sol. Energy Mater. Sol. Cells*, 1994, **33**, 475.
26 K. Vinodgopal, D. E. Wynkop and P. V. Kamat, *Environ. Sci. Technol.*, 1996, **30**, 1660.
27 B. O'Regan and M. Grätzel, *Nature*, 1991, **353**, 737.
28 R. Grunwald and H. Tributsch, *J. Phys. Chem. B*, 1997, **101**, 5552.
29 Q. Qu, J. C. Zhao and T. Sheu, *J. Mol. Catal. A: Chem.*, 1998, **129**, 257.
30 R. Vogel, P. Hoye and H. Weller, *Chem. Phys. Lett.*, 1990, **174**, 241.
31 D. Liu and P. V. Kamat, *J. Phys. Chem.*, 1993, **97**, 10 769.
32 A. Ennaoui, S. Fiechter, H. Tributsch, M. Giersig, R. Vogel and H. Well, *J. Electrochem. Soc.*, 1992, **139**, 2514.
33 M. Ashokkumar, A. Kndo, N. Saito and T. Sakata, *Chem. Phys. Lett.*, 1994, **299**, 383.
34 S. A. Feriedberg and D. L. Bark, *Phys. Rev.*, 1955, **98**, 1200.
35 E. F. Westrum and J. E. Goldman, *J. Phys. Chem.*, 1957, **61**, 761.
36 Z. H. Yuan, W. You, J. H. Jia and L. D. Zhang, *Chin. Phys. Lett.*, 1998, **15**, 535.
37 L. G. J. De Harrt and G. Blasse, *J. Electrochem. Soc.*, 1985, **132**, 2933.
38 J. J. Liu, G. X. Lu, H. L. He, H. Tan, T. Xu and K. Xu, *Mater. Res. Bull.*, 1996, **31**, 1049.
39 X. Y. Li, S. B. Li and G. X. Lie, *J. Mol. Catal.*, 1996, **31**, 187 (in Chinese).
40 M. Seki, T. Sato and S. Usui, *J. Appl. Phys.*, 1988, **63**, 1424.
41 D. Bahnemann, A. Henglein, J. Lilie and L. Spanhel, *J. Phys. Chem.*, 1984, **88**, 709.
42 Z. H. Yuan and L. D. Zhang, *Nanostruct. Mater.*, 1998, **10**, 1127.
43 T. Sato, K. Haneda, M. Seki and T. Iijima, *Appl. Phys. A*, 1990, **50**, 13.
44 B. Jeyadevan, K. Tahji and K. Nakatsuka, *J. Appl. Phys.*, 1994, **76**, 6325.
45 M. S. Kaliszewsk and A. H. Heuer, *J. Am. Ceram. Soc.*, 1990, **73**, 1504.
46 D. C. Hague and M. J. Mayo, *J. Am. Ceram. Soc.*, 1994, **77**, 1957.
47 X. Z. Ding, L. Liu, X. M. Ma, Z. Z. He and Y. Z. He, *J. Mater. Sci. Lett.*, 1994, **13**, 462.